THE JOURNAL OF BIOLOGICAL CHEMISTRY VOL. 282, NO. 40, pp. 29305–29313, October 5, 2007

Raft-dependent Endocytosis of Autocrine Motility Factor Is Phosphatidylinositol 3-Kinase-dependent in Breast Carcinoma Cells*

Received for publication, May 16, 2007, and in revised form, July 25, 2007 Published, JBC Papers in Press, August 8, 2007, DOI 10.1074/jbc.M704069200

Liliana D. Kojic[‡], Bharat Joshi[‡], Patrick Lajoie[‡1], Phuong U. Le[§], Michael E. Cox[¶], Dmitry A. Turbin[‖], Sam M. Wiseman[¶‖2], and Ivan R. Nabi[‡3]**

*From the [‡]Department of Cellular and Physiological Sciences, Life Sciences Institute, University of British Columbia, Vancouver, British Columbia V6T 1Z3, [§]National Research Council, Biotechnology Research Institute, Montreal, Quebec H4P 2R2, [¶]Prostate Research Centre, British Columbia Cancer Agency and University of British Columbia, Vancouver, British Columbia V6H 3Z6, [‖]Genetic Pathology Evaluation Centre, Department of Pathology, Vancouver General Hospital, British Columbia Cancer Agency, and University of British Columbia, Vancouver, British Columbia V6H 3Z6, and the **Department of Surgery, St. Paul's Hospital/University of British Columbia, Vancouver, British Columbia V6T NZ, Canada*

Autocrine motility factor (AMF) is internalized via a receptor-mediated, dynamin-dependent, cholesterol-sensitive raft pathway to the smooth endoplasmic reticulum that is negatively regulated by caveolin-1. Expression of AMF and its receptor (AMFR) is associated with tumor progression and malignancy; however, the extent to which the raft-dependent uptake of AMF is tumor cell-specific has yet to be addressed. By Western blot and cell surface fluorescence-activated cell sorter (FACS) analysis, AMFR expression is increased in tumorigenic MCF7 and metastatic MDA-231 and MDA-435 breast cancer cell lines relative to dysplastic MCF10A mammary epithelial cells. AMF uptake, determined by FACS measurement of protease-insensitive internalized fluorescein-conjugated AMF, was increased in MCF7 and MDA-435 cells relative to MCF-10A and caveolin-1-expressing MDA-231 cells. Uptake of fluorescein-conjugated AMF was dynamin-dependent, methyl-β-cyclodextrin- and genistein-sensitive, reduced upon overexpression of caveolin-1 in MDA-435 cells, and increased upon short hairpin RNA reduction of caveolin-1 in MDA-231 cells. Tissue microarray analysis of invasive primary human breast carcinomas showed that AMFR expression had no impact on survival but did correlate significantly with expression of phospho-Akt. Phospho-Akt expression was increased in AMF-internalizing MCF7 and MDA-435 breast carcinoma cells. AMF uptake in these cells was reduced by phosphatidylinositol 3-kinase inhibition but not by regulators of macropinocytosis such as amiloride, phorbol ester, or actin cytoskeleton disruption by cytochalasin D. The raft-dependent endocytosis of AMF therefore follows a distinct phosphatidylinositol 3-kinase-dependent pathway that is up-regulated in more aggressive tumor cells.

Autocrine motility factor (AMF)[4] is secreted by and stimulatory to tumor cells. AMF exhibits sequence identity to phosphoglucose isomerase, a glycolytic enzyme that also exhibits neurokine and lymphokine activities (1). AMFR expression is associated with poor survival and prognosis of patients with gastric, colorectal, bladder, and esophageal carcinomas, cutaneous malignant melanoma, and pulmonary adenocarcinoma (2–8). Importantly, in many of these studies, AMFR was absent or present at significantly reduced levels in adjacent normal tissue. Recently, a genome-wide analysis identified AMFR as one of 189 genes that present a high frequency of intragenic mutations in breast cancer (9). Altered expression of AMFR is therefore associated with breast tumor progression and metastasis.

AMFR localizes to cell surface caveolae and internalizes AMF to the smooth endoplasmic reticulum via a dynamin-dependent, raft-mediated endocytic pathway negatively regulated by caveolin-1 (Cav1) (10–12). Multiple raft-dependent pathways have been described that vary in their dependence on expression of Cav1 and dynamin-2 (13, 14). The AMF pathway can be distinguished from the caveolae/raft-dependent endocytosis of SV40 virus to the endoplasmic reticulum (15) and of cholera toxin b-subunit to the Golgi apparatus by the insensitivity of its uptake to brefeldin A, nocodazole, and a 20 °C temperature block (11). Reduced expression of Cav1 upon transformation of NIH-3T3 cells with *ras* or *abl* oncogenes is associated with increased AMF uptake (12). Conversely, AMF transfection of NIH-3T3 cells induces enhanced transformation and survival via PI3K/Akt signaling and Cav1 down-regulation (16). This suggests that AMF/AMFR expression and signaling are inversely related to Cav1 expression during tumor progression. However, AMF endocytosis in human tumor cells has yet to be

* This work was supported in part by a grant from the Canadian Institutes of Health Research. The costs of publication of this article were defrayed in part by the payment of page charges. This article must therefore be hereby marked "*advertisement*" in accordance with 18 U.S.C. Section 1734 solely to indicate this fact.

[1] Research student of the Terry Fox Foundation through an award from the National Cancer Institute of Canada.

[2] A Michael Smith Scholar.

[3] Canadian Institutes of Health Research Investigator. To whom correspondence should be addressed: Dept. of Cellular and Physiological Sciences, University of British Columbia, 2350 Health Sciences Mall, Vancouver, British Columbia V6T 1Z3, Canada. E-mail: irnabi@interchange.ubc.ca.

[4] The abbreviations used are: AMF, autocrine motility factor; AMF-FITC, fluorescein-conjugated AMF; AMFR, autocrine motility factor receptor; Cav1, caveolin-1; ER, estrogen receptor; FACS, fluorescence-activated cell sorter; HER2, herceptin2; Tf-FITC, FITC-conjugated transferrin; mβCD, methyl-β-cyclodextrin; PI3K, phosphatidylinositol 3-kinase; PR, progesterone receptor; TMA, tissue microarray; TPA, phorbol ester12-*O* tetradecanoylphorbol 13-acetate; shRNA, short hairpin RNA; MFI, mean fluorescence intensity; RT, reverse transcription; mAb, monoclonal antibody.

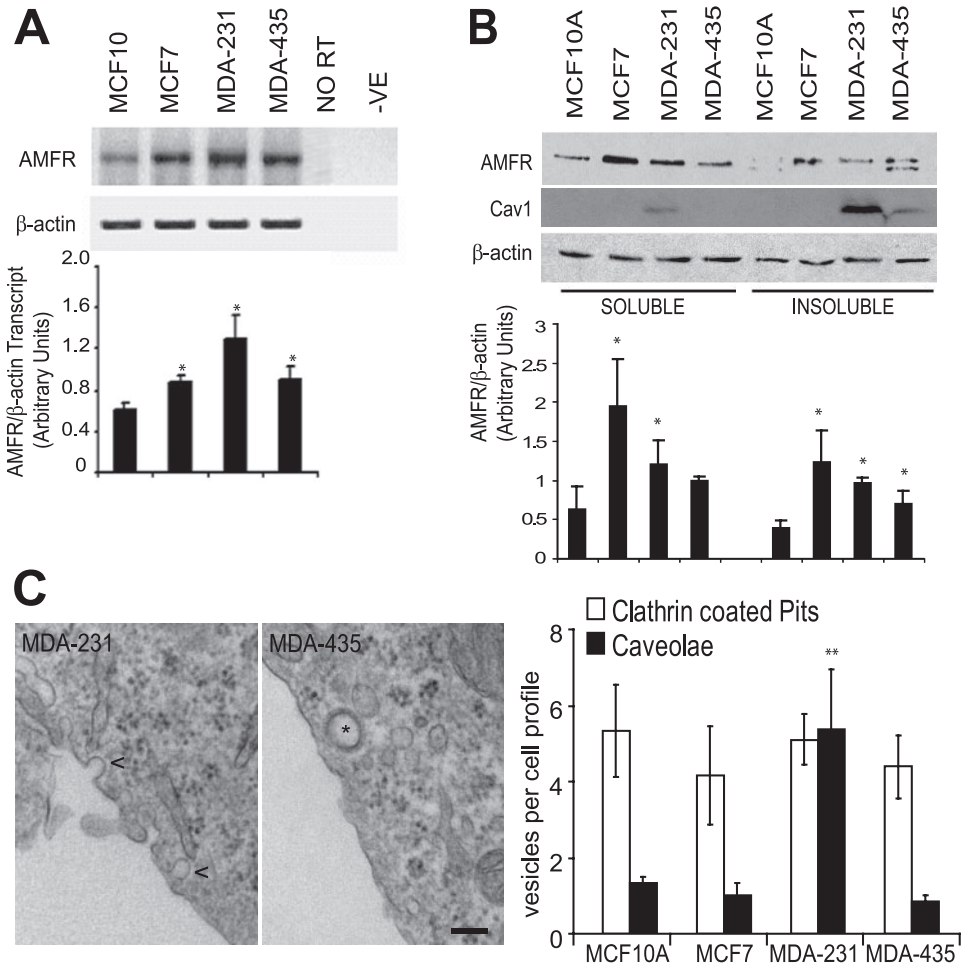

FIGURE 1. **AMFR and caveolin expression in human breast tumor cells.** *A,* mRNA was prepared from MCF10A, MCF7, MDA-231, and MDA-435 breast cell lines and analyzed for AMFR and β-actin expression by semi-quantitative RT-PCR (*RT*)-*VE,* negative control. *B,* Nonidet P-40 soluble and insoluble fractions from MCF10A, MCF7, MDA-231, and MDA-435 breast cell lines were analyzed by Western blot for AMFR, Cav1/2, and β-actin. The *graph* presents densitometric analysis for AMFR expression relative to β-actin. *C,* representative electron microscopy images of the plasma membrane of MDA-231 and MDA-435 cells are shown and the number of plasma membrane caveolae (*arrowheads, white bars*) and clathrin-coated pits (*asterisk, black bars*) quantified in MCF10A, MCF7, MDA-231, and MDA-435 cells. *, $p < 0.05$; **, $p < 0.01$.

studied, and factors that promote the raft-dependent endocytosis of AMF have not been identified.

In this study, we show that AMF internalization is reduced in dysplastic MCF10A mammary cells relative to tumorigenic and metastatic tumor cell lines and that Cav1 is a critical regulator of the raft-dependent endocytosis of AMF in breast carcinoma cells. Tissue microarray analysis (TMA) of AMFR expression identified a highly significant association with p-Akt. AMF stimulates p-Akt expression, and PI3K inhibition prevents raft-dependent AMF uptake in breast carcinoma cells. PI3K is therefore identified as a positive regulator of the AMF raft pathway, indicative of a feedback loop linking AMFR signaling through PI3K to AMF uptake.

EXPERIMENTAL PROCEDURES

Cells, Antibodies, and Reagents—MCF7, MDA-231, MDA-435, and MCF10A human breast cell lines (ATCC, Manassas, VA) were maintained in complete RPMI 1640 medium containing 10% FBS. Monoclonal rat IgM anti-AMFR (3F3A) was used as ascites fluid (17). Rabbit anti-Cav1/2 and mouse anti-Cav1 antibody were from Transduction Laboratories; rabbit anti-p-Akt and Akt were from Cell Signaling (Danvers, MA); Alexa488- and Alexa647-conjugated secondary antibodies, Alexa568-conjugated phalloidin, and rabbit anti-FITC antibodies were from Molecular Probes (Eugene, OR), and rhodamine red-X anti-rat IgM was from Jackson ImmunoResearch (West Grove, PA). Commercial rabbit phosphoglucose isomerase (referred to as AMF) was purchased from Sigma (P-9544) and conjugated to FITC using fluorescein-EX protein labeling kit (Molecular Probes). Monoclonal anti-β-actin, methyl-β-cyclodextrin (mβCD), genistein, FITC-conjugated transferrin (Tf-FITC), propidium iodide, goat serum, and Pronase were from Sigma, and LY294002 was from Calbiochem.

Cav1 shRNA Lentiviral Constructs—Core sequences for Cav1 shRNA constructs (5′-CTGTTCCCATCCGGGAACAGGGCAACAT-3′) were cloned into pSHAG-1 plasmid (Dr. G. Hannon, Cold Spring Harbor, NY), and the shRNA cassette was transferred into pLenti6/BLOCK-iT™-DEST (Invitrogen) that carries a blasticidin selection marker. Lentiviral vector from conditioned media of HEK293T cells transfected with Cav1 shRNA-pLenti6/BLOCK-iT™-DEST (18) was used to infect MDA-231 cells. A pooled population of blasticidin-selected MDA-231 cells exhibiting maximal Cav1 suppression was used for subsequent experiments.

Western Blots and RT-PCR—Cell lysates were prepared as described (19) and centrifuged for 15 min at 13,000 rpm at 4 °C. Supernatant and pellet, the latter passed 20 times through a 21.5-gauge needle, were separated on 10% SDS-PAGE, electroblotted onto nitrocellulose membranes, and revealed with the indicated primary antibodies, horseradish peroxidase-conjugated secondary antibodies, and chemiluminescence. Band intensity was quantified by densitometry relative to β-actin.

Total RNA was extracted by the TRIzol method, and RT-PCR was performed following standard protocols using SuperScript III reverse transcriptase (Invitrogen), oligo(dT), and primers for AMFR (5′-ATGCCGCTGCTCTTCCTCGAGCGC-3′; 5′-TCAACCGAAAAACTCGGCAGCCAGCTC-3′) and β-actin (5′-GCCCTTTCTCACTGGTTCTC-3′; 5′-CTTTACACCAGCCTCATGGC-3′).

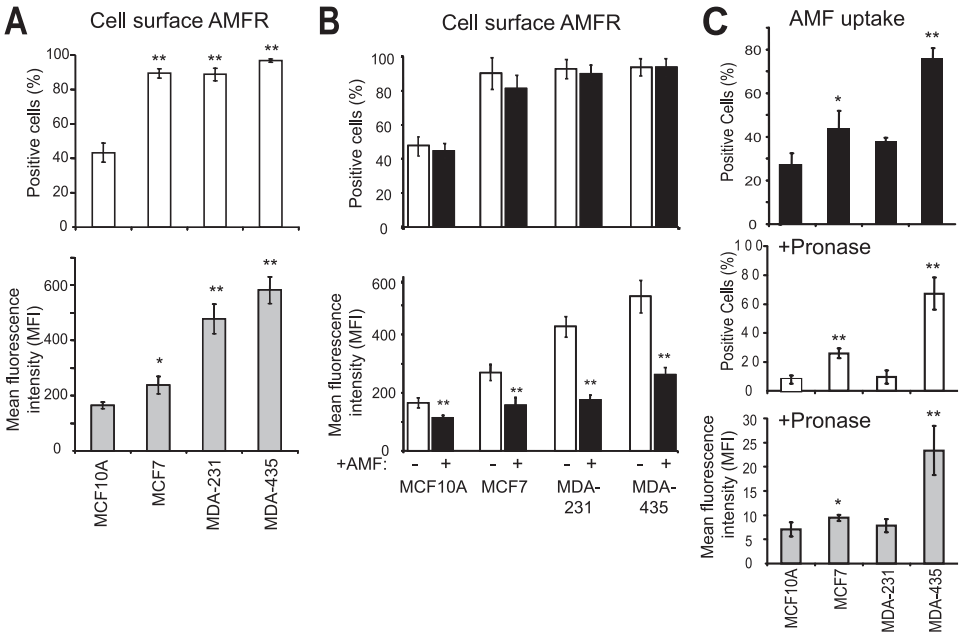

FIGURE 2. **Cell surface expression of AMFR and internalization of AMF in human breast tumor cells.** *A*, surface AMFR expression of MCF10A, MCF7, MDA-231, and MDA-435 cells stained with 3F3A anti-AMFR mAb followed by Alexa647-conjugated secondary antibody was analyzed by FACS (*top graph*, percent positive cells; *bottom graph*, MFI). *B*, MCF10A, MCF7, MDA-231, and MDA-435 cells were incubated for 60 min at 4 °C in the absence (*white bars*) or presence (*black bars*) of 1 mg/ml AMF prior to cell surface labeling with 3F3A anti-AMFR mAb followed by Alexa647-conjugated secondary antibody and FACS analysis. *C*, MCF10A, MCF7, MDA-231, and MDA-435 breast cells were incubated for 30 min at 37 °C in the presence of AMF-FITC. FACS analysis of AMF-FITC uptake was performed before (*top*) and after (*middle, bottom*) a 15-min incubation with Pronase (400 μg/ml). $n \geq 3$; mean ± S.E.; *, $p < 0.05$; **, $p < 0.005$ relative to MCF10A (*A* and *C*) or control (*B*).

Immunofluorescence, FACS, and Electron Microscopy—Immunofluorescence, FACS, and electron microscopy were performed as described (10, 12). For uptake analysis, adherent cells were incubated with 25 μg/ml AMF-FITC or 15 μg/ml Tf-FITC for 30 min at 37 °C. For FACS analysis, cell surface-bound conjugate was removed with Pronase (400 μg/ml) for 15 min. Flow cytometry measurements of at least 50,000 cells used Cellquest software on a FACSCalibur (BD Biosciences). Adenoviral constructs and infection were as described (12, 20).

Statistical Analysis—RT-PCR, Western blots, immunofluorescence, and FACS experiments were reproduced at least three times, and representative blots and images are presented. FACS experiments were performed in duplicate. Unless otherwise stated, all values are presented as mean ± S.E. of at least three independent experiments. Statistical significance was evalu-

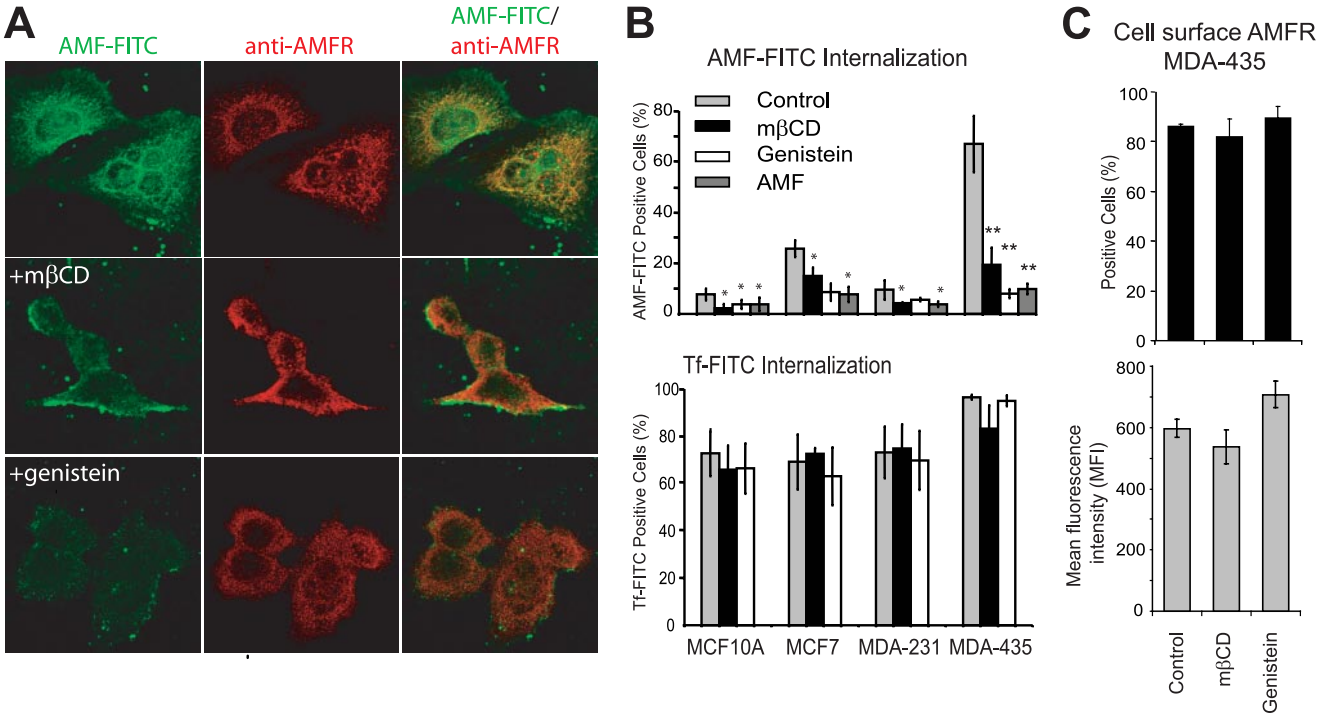

FIGURE 3. **Internalization of AMF to the smooth endoplasmic reticulum of invasive breast cancer cells is raft-dependent.** *A*, MDA-435 cells, pretreated for 30 min with 5 mM mβCD (+*mβCD*; *middle row*) or 100 μg/ml genistein (+*genistein*; *bottom row*), were incubated with 25 μg/ml AMF-FITC for 30 min prior to fixation. AMF-FITC was revealed with rabbit anti-FITC (*green*) and the smooth endoplasmic reticulum with 3F3A anti-AMFR monoclonal antibody (*red*) followed by appropriate secondary antibodies. *B*, MCF10A, MCF7, MDA-231, and MDA-435 breast cells were pretreated for 30 min with 5 mM mβCD, 100 μg/ml genistein, or an excess of unconjugated AMF (1 mg/ml) and then incubated with AMF-FITC (*top*) or Tf-FITC (*bottom*), followed by incubation with Pronase and FACS analysis ($n \geq 3$; mean ± S.E.; *, $p < 0.05$; **, $p < 0.005$ relative to control). *C*, surface AMFR expression of MDA-435 cells treated for 30 min with 5 mM mβCD or 100 μg/ml genistein were stained with 3F3A anti-AMFR mAb followed by Alexa647-conjugated secondary antibody and analyzed by FACS (*top graph*, percent positive cells; *bottom graph*, MFI).

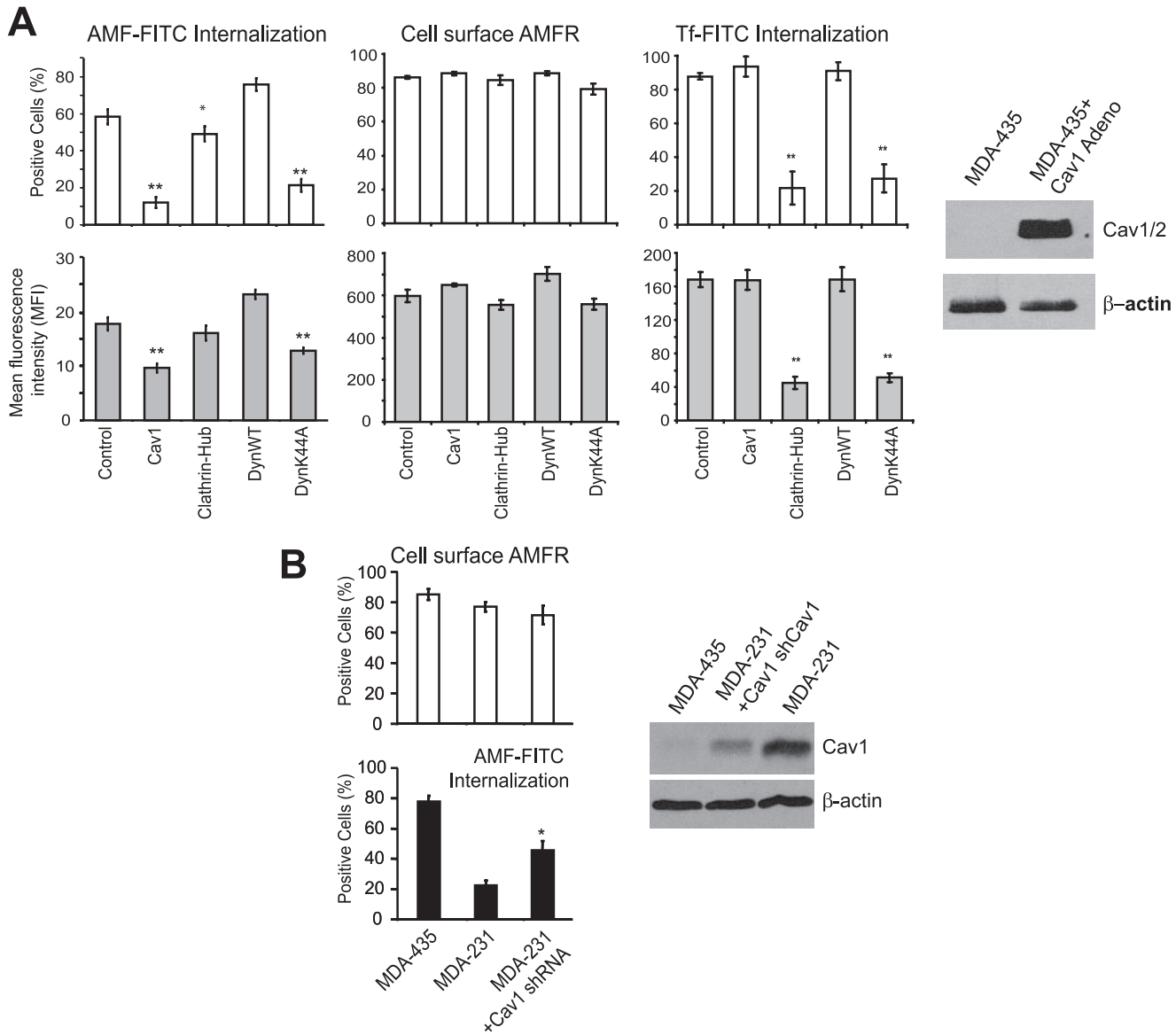

FIGURE 4. **Cav1 is a negative regulator of AMF uptake in invasive breast cancer cells.** *A,* MDA-435 cells were infected with adenoviruses expressing Cav1, clathrin hub, wild-type dynamin-1 (*DynWT*) or mutant dynamin-1 K44A (*DynK44A*). After 48 h, AMF-FITC uptake, cell surface AMFR expression with the 3F3A mAb, and Tf-FITC uptake were assessed by FACS (*top graph,* percent positive cells; *bottom graph,* MFI). Cell lysates of uninfected and Cav1 adenovirus-infected cells were probed with polyclonal anti-caveolin and anti-β-actin antibodies (*right*). *B,* MDA-435, MDA-231 and stable lentiviral-infected Cav1 shRNA MDA-231 cells were analyzed for AMFR surface expression (*top panel*) and AMF uptake (*bottom panel*) by FACS and for Cav1 expression levels by Western blot (*right panel*). ($n \geq 3$; mean ± S.E.; *, $p < 0.05$; **, $p < 0.001$, relative to control (*A*) or MDA-231 (*B*)).

ated using the Student's *t* test for paired comparison; $p < 0.05$ was considered significant.

Human Breast Tissue Microarrays—438 sequential archival cases of invasive breast carcinoma, with available paraffin blocks, that had undergone treatment at Vancouver General Hospital between 1974 and 1995 were identified for TMA construction (21) with adequate tissue present for interpretation of 370 cases. The study was approved by the Clinical Research Ethics Board of the University of British Columbia. Antibodies used and antigen retrieval methodologies are summarized in Fig. 5*A*. Semi-quantitative scoring of TMA sections stained for ER and PR (22), HER2 (23), and p-Akt (24) was as described previously. AMFR was scored positive (1+) if any invasive carcinoma cell staining was observed. For statistical analyses, score data were binarized using ≥10% cutoffs for ER and PR and a score of 1+ for AMFR and 2+ (equivalent to strong 3+ staining when utilizing the Herceptest) for HER2. TMA slides were digitized using a BLISS slide scanner (Bacus Laboratories, Inc., Chicago) and connected to a relational data base. They are publicly available on line. All samples were evaluated and scored, from scanned images on a computer monitor, by two pathologists blinded to patient clinical data.

Clinical data on all patients was retrospectively collected from patient hospital charts. Median patient follow-up was 15 years, and all patients had newly diagnosed stage I–III invasive breast cancer. Clinicopathologic data collected included patient age and sex, lymph node status (negative *versus* positive), tumor size, tumor grade, tumor histology, patient follow-up, and survival. All data were logged onto a standardized score

A

Antibody	Isotype	Clone	Company	Catalogue #	AgR	Concentration
AMFR	Rat IgM	3F3A	I. R. Nabi	X	Citrate buffer pH 6.0	1 in 50
HER2	Rabbit polyclonal	X	DAKO	A485	Steam 20min, TRS	1 in 500
ER	Rabbit monoclonal	SP1	Labvision	RM9101	Citrate buffer pH 6.0	1 in 200
PR	Rabbit monoclonal	SP2	Labvision	RM9102	Citrate buffer pH 6.0	1 in 400
PAKT	Rabbit polyclonal	SER473	Cell Signaling Tech	9277	EDTA buffer pH 8.0	1 in 2

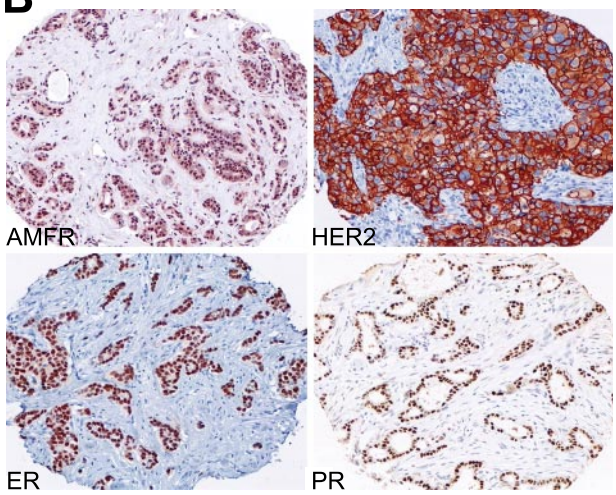

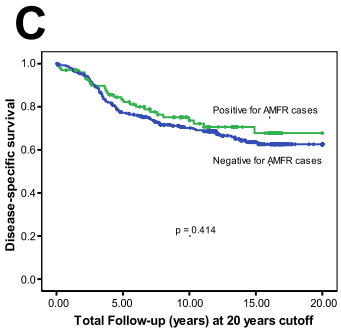

D

Biomarker	Correlation Coefficient (Spearman's rho)	P value (2-tailed)
Tumour Size	-0.038	0.464
Histologic Grade	-0.022	0.694
Nodal Status	-0.136	0.015
Estrogen Receptor	-0.004	0.943
Progesterone Receptor	-0.126	0.025
HER2	-0.004	0.942
Phospho-Akt	0.213	0.000065

FIGURE 5. **AMFR expression in primary human breast tumor tissues.** A breast tumor tissue microarray containing 438 formalin-fixed, paraffin-embedded breast tissue samples of invasive nonmetastatic breast tumors was stained as described under "Experimental Procedures." *A,* characteristics of antibodies utilized for immunohistochemistry are presented as a *table. B,* representative tissue cores exhibiting strong expression of AMFR, HER2, ER, and PR are shown. *C,* Kaplan-Meier survival curves were determined based on AMFR expression for 370 interpretable cases. *D,* correlation table for AMFR is presented for the same cohort.

sheet matching each TMA section (Microsoft Excel, Redmond, WA), processed utilizing TMA-Deconvoluter 1.07 software (25), and analyzed by SPSS 11.0 statistical software (SPSS, Chicago, IL). Correlation analysis used the bivariate two-tailed Spearman nonparametric correlation test. Differences were considered significant when $p < 0.05$. The Kaplan-Meier method was utilized for survival analysis with log rank test to determine significance in survival differences. For the multivariate analysis, we used a proportional hazards model (Cox regression model).

RESULTS

AMFR Expression and Internalization in Human Mammary Cell Lines—AMFR transcript and protein levels were significantly increased in MCF7, MDA-231, and MDA-435 breast cancer cell lines relative to dysplastic epithelial MCF10A cells (Fig. 1*A*). Protein, but not transcript, levels of AMFR were increased in MCF7 cells relative to metastatic MDA-231 and MDA-435 cells. By Western blot, AMFR was detected in both Nonidet P-40 soluble and insoluble fractions and Cav1 predominantly in the insoluble fraction (Fig. 1*B*). Cav1 levels were highest in MDA-231 cells, lesser in MDA-435 cells, and barely detectable in MCF10A and MCF7 cells (Fig. 1*B*). Higher expression of Cav1 in MDA-231 cells was associated with a significantly increased number of caveolae (Fig. 1*C*).

FACS analysis showed that fewer dysplastic MCF10A cells were positive for surface AMFR expression relative to the three cancer cell lines; metastatic MDA-435 and MDA-231 presented 2–3-fold increased mean fluorescence intensity (MFI) for surface AMFR expression relative to MCF7 and dysplastic MCF10A cell lines (Fig. 2*A*). Cell surface binding of anti-AMFR was efficiently competed by preincubation of the cells with AMF at 4 °C demonstrating, as reported previously (17), that the 3F3A anti-AMFR antibody is specific for the AMF receptor (Fig. 2*B*).

When incubated with cells for 30 min at 37 °C, AMF-FITC showed increased association with MDA-435 cells relative to the other breast cell lines by FACS (Fig. 2*C*). Upon removal of cell surface-bound AMF-FITC by Pronase, MDA-435 cells showed significant uptake of AMF-FITC both in terms of positive cell number and MFI. AMF-FITC uptake was significantly increased in MCF7 relative to MCF10A and MDA-231 cells but reduced relative to MDA-435 cells.

Regulation of AMFR Uptake by Cav1 in Breast Cancer Cells—Internalization of AMF-FITC to the anti-AMFR-labeled smooth endoplasmic reticulum is inhibited by cholesterol extraction with mβCD and the tyrosine kinase inhibitor genistein (Fig. 3*A*). FACS analysis confirmed that these inhibitors of caveolae/raft-dependent endocytosis inhibited AMF-FITC internalization without impacting on clathrin-dependent uptake of Tf-FITC (Fig. 3*B*). AMF uptake in these cell lines is receptor-mediated as a 10-fold excess of unlabeled AMF competed for AMF-FITC uptake (Fig. 3*B*). Neither mβCD nor genistein treatment impacted on cell surface AMFR expression (Fig. 3*C*).

Adenoviral expression of Cav1 and mutant dynamin-1 K44A, but not clathrin hub or wild-type dynamin, significantly inhibited AMF-FITC uptake in MDA-435 cells without impacting cell surface AMFR expression (Fig. 4*A*). As a control, adenoviral expression of the clathrin hub and mutant dynamin-1 K44A, but not Cav1 or wild-type dynamin-1, was found to inhibit clathrin-dependent uptake of Tf-FITC (Fig. 4*A*). Conversely, lentiviral infection of MDA-231 cells with Cav1 shRNA, reducing Cav1 levels by ~80%, resulted in a 2-fold increase in AMF

uptake (Fig. 4*B*). Cav1 expression therefore negatively regulates the clathrin-independent, dynamin-dependent, raft-dependent uptake of AMF in invasive breast cancer cells.

Tissue Microarray Analysis of Invasive Human Breast Carcinomas—From TMA analysis (Fig. 5), 99 of 370 interpretable cases (27%) of invasive breast cancer expressed AMFR. Increased AMFR expression was not associated ($p = 0.414$) with disease-specific survival (Fig. 5*C*). No correlations were found between AMFR expression and tumor HER2, ER status, tumor size, or histologic grade. AMFR had a weak negative correlation with tumor PR status ($p = 0.025$) and axillary lymph node status ($p = 0.015$) (Fig. 5*D*). Interestingly, AMFR expression showed a highly significant correlation ($p = 0.000065$) with p-Akt, previously scored on the same breast cancer TMA (24).

Raft-dependent Endocytosis of AMF Is PI3K-dependent—The high degree of correlation of AMFR and p-Akt in the TMA analysis led us to assess p-Akt expression in the breast cancer cell lines. As seen in Fig. 6*A*, basal p-Akt levels are elevated in MCF7 and MDA-435 relative to MCF10A and MDA-231 cells. Furthermore, in MDA-435 cells, AMF induced Akt phosphorylation after 2 h (Fig. 6*B*), consistent with the up-regulation of p-Akt in stable AMF-transfected NIH-3T3 cells (16). Treatment with genistein had no effect on pAkt phosphorylation in MDA-435 and MCF7 cells indicating that decrease of AMF uptake by genistein is not due to PI3K inhibition (Fig. 6*C*).

Increased p-Akt expression corresponds to the increased AMF uptake detected in MDA-435 cells and, to a lesser extent, in MCF7 cells (Fig. 2). Pretreatment with the PI3K inhibitor, LY294002, for 60 min inhibited Akt phosphorylation (Fig. 7*A*) and, when added prior to addition of AMF-FITC, significantly inhibited AMF uptake in MCF7 and MDA-435 cells (Fig. 7*B*). PI3K inhibition affected neither AMFR surface expression nor uptake of Tf-FITC (Fig. 7*B*). PI3K has been described as a regulator of macropinocytosis (26–28). However, AMF uptake was not affected by inhibitors of macropinocytosis such as amiloride or actin disruption with cytochalasin D nor stimulated by the phorbol ester 12-*O*-tetradecanoylphorbol 13-acetate (TPA) (Fig. 7, *C* and *D*).

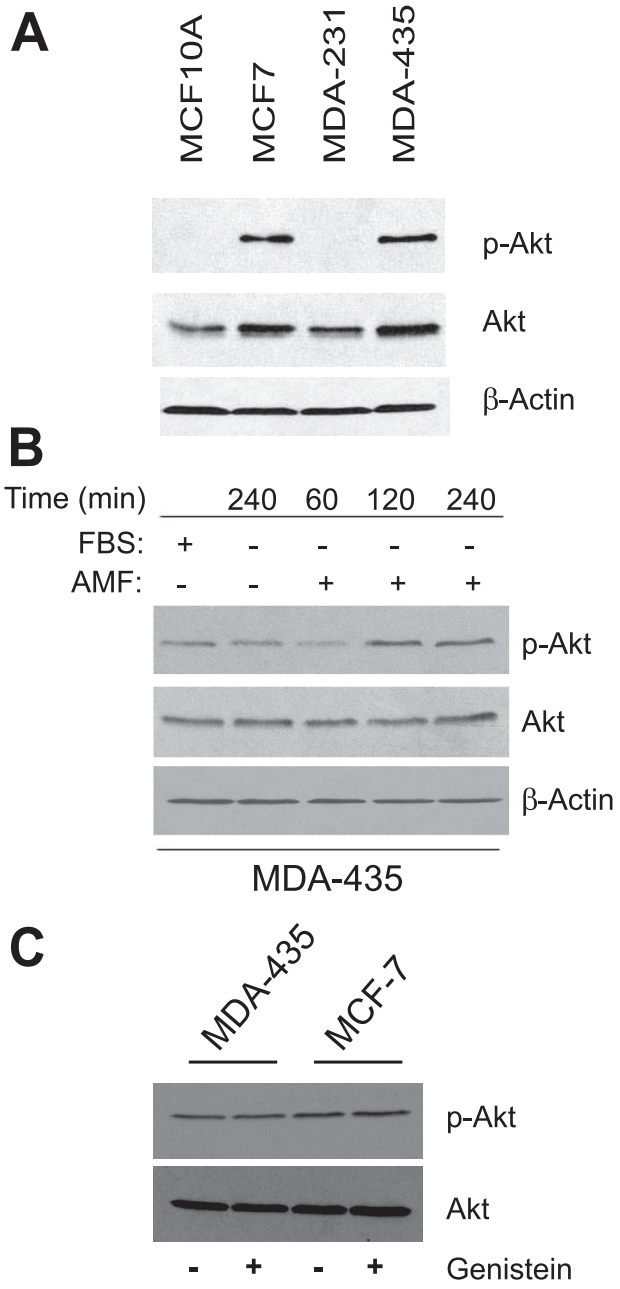

FIGURE 6. **AMF stimulates pAkt phosphorylation in MDA-435 cells.** *A,* Nonidet P-40-soluble fractions from MCF10A, MCF7, MDA-231, and MDA-435 breast cell lines were analyzed by Western blot for p-Akt, Akt, and β-actin. *B,* MDA-435 cells were grown in serum-containing media (+*FBS*) or serum-starved and incubated in fresh media without AMF for 240 min or with AMF for 60, 120, and 240 min, and Nonidet P-40-soluble fractions analyzed by Western blot for p-Akt, Akt, and β-actin. *C,* MDA-435 and MCF7 cells were incubated with or without 100 μg/ml genistein for 30 min, as indicated, and Nonidet P-40-soluble fractions were analyzed by Western blot for p-Akt and Akt.

DISCUSSION

AMFR expression was reduced in dysplastic MCF10A cells relative to breast cancer cell lines. AMFR is expressed both at the cell surface and within the smooth endoplasmic reticulum (29). Reduced expression of AMFR by Western blot contrasted with its increased mRNA transcript and cell surface expression by FACS in metastatic MDA-231 and MDA-435 cells relative to the nonmetastatic MCF7 cells. AMFR is a critical ubiquitin-protein isopeptide ligase involved in ER-associated degradation and can target itself for degradation by the proteasome (30). The role of the ER-associated degradation function of AMFR in tumor cells remains uncertain. However, our data suggest that the cell surface expression of AMFR is more closely associated with its role in metastasis.

Uptake of exogenous AMF was detected selectively in tumorigenic MCF7 and metastatic MDA-435 breast tumor cells (31), consistent with increased AMFR internalization in Ras-transformed NIH-3T3 and metastatic B16-F1 melanoma cells (12, 32). In these, uptake of protease-sensitive AMF-FITC is clathrin-independent, dynamin-dependent, and cholesterol- and tyrosine kinase-sensitive. AMF uptake in these breast cancer cell lines therefore follows the same caveolae/raft-dependent pathway to the AMFR-positive smooth endoplasmic reticulum as reported previously in other cell types (10, 12, 33). Reduced uptake of AMF in metastatic MDA-231 cells was associated with increased expres-

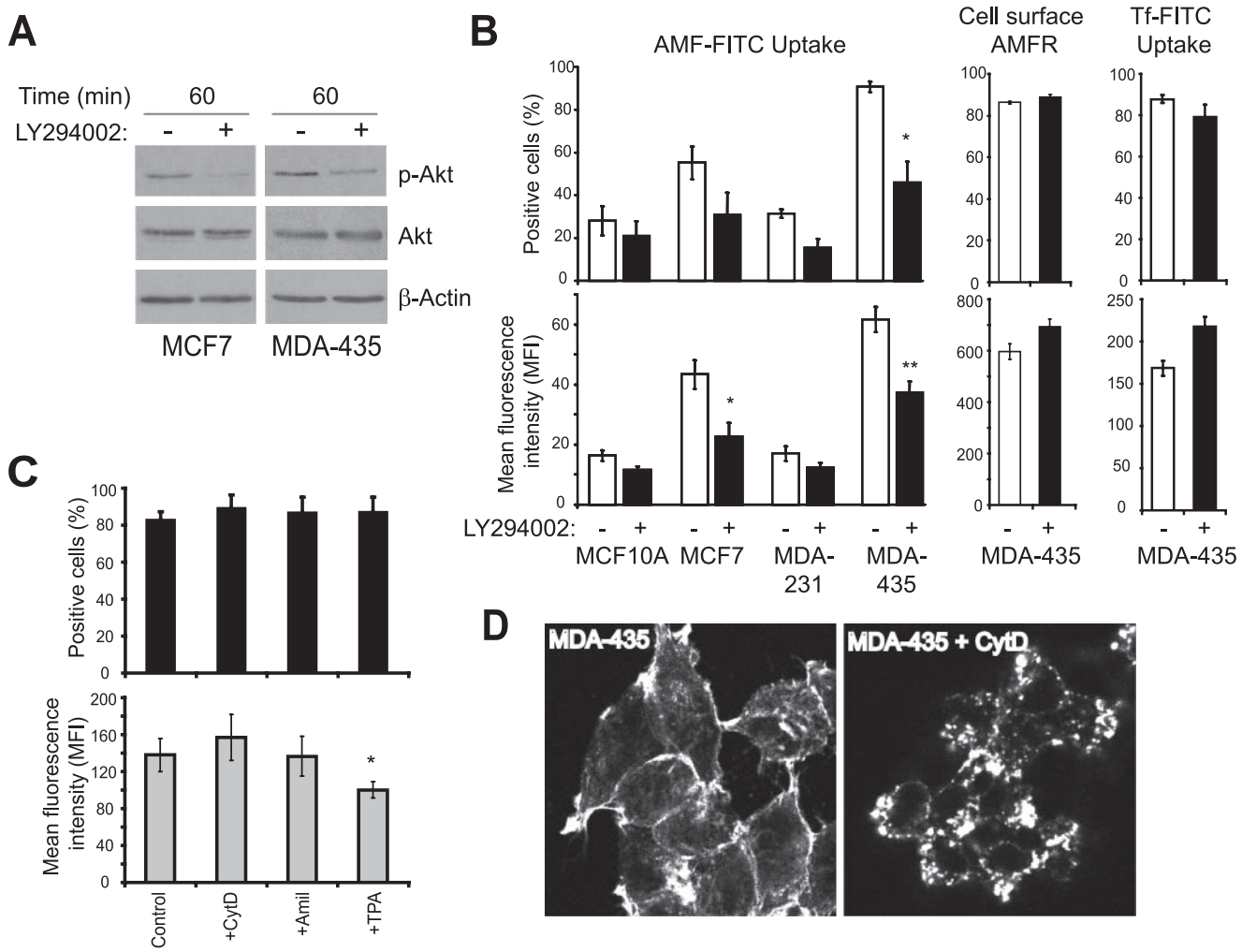

FIGURE 7. **Raft-dependent endocytosis of AMF is PI3K-dependent.** *A,* MCF7 and MDA-435 cells were incubated with or without 50 μM LY294002 for 60 min, and Nonidet P-40-soluble fractions were analyzed by Western blot for p-Akt, Akt, and β-actin. *B,* MCF10A, MCF7, MDA-231, and MDA-435 breast cells were pretreated for 30 min in the absence (*white bars*) or presence (*black bars*) of 50 μM LY294002 after which AMF-FITC uptake was assessed by FACS. For untreated and LY294002-treated MDA-435 cells, cell surface AMFR expression and Tf-FITC uptake were also determined by FACS ($n = 3$; mean $\pm$ S.E.; *, $p < 0.05$; **, $p < 0.001$). *C,* MDA-435 cells were pretreated with 100 μM amiloride or 10 μM cytochalasin D for 30 min or 1 μg/ml TPA for 60 min after which AMF-FITC uptake was assessed by FACS ($n = 3$; mean $\pm$ S.E.; *, $p < 0.05$). *D,* F-actin of untreated, cytochalasin D- and TPA-treated paraformaldehyde-fixed MDA-435 cells, as indicated, was labeled with Alexa568-conjugated phalloidin and imaged with the $\times$100 objective of an Olympus FV100 confocal microscope.

sion of Cav1. Cav1 overexpression and Cav1 shRNA in metastatic MDA-435 and MDA-231 cells, respectively, identifies Cav1 as a critical, negative regulator of AMF uptake in these invasive cancer cells.

The high degree of correlation of AMFR and p-Akt (24) on the same breast tumor TMA (Fig. 5) led us to assess whether PI3K regulates AMF uptake. In MDA-435 cells, AMF induced Akt phosphorylation and PI3K regulated AMF uptake. In addition, p-Akt expression was higher in AMF internalizing MCF7 and MDA-435 cells but not in the poorly internalizing, Cav1 expressing MDA-231 cells (Fig. 6*A*). Multiple kinases have been shown to regulate caveolae-mediated SV40 uptake (34), and the fact that genistein inhibits AMF uptake but does not affect Akt phosphorylation argues that other kinases are involved in the raft-dependent endocytosis of AMF. AMF stimulation of p-Akt phosphorylation in MDA-435 cells was detectable after only 2 h, far longer than the short (<5 min) time of AMF delivery to the smooth endoplasmic reticulum (11). It is therefore not clear whether AMF-dependent PI3K activation autoregulates its endocytosis or whether AMF uptake is required for its activation of PI3K.

Multiple pathways of raft-dependent endocytosis have been described, including dynamin-dependent, caveolae/raft-mediated and dynamin-independent, noncaveolar pathways (13, 14). The latter includes PI3K-, raft-dependent but dynamin-independent macropinocytosis (13). However, inhibition of the protease-sensitive uptake of AMF by the dynamin 1 K44A mutant demonstrates that the dynamin sensitivity of AMF uptake occurs at the cell surface and not at a subsequent internal site. Furthermore, AMF uptake was not affected by regulators of macropinocytosis identifying the raft-dependent uptake of AMF as a distinct PI3K-dependent raft endocytic pathway. PI3K inhibitors have been shown to inhibit uptake of fluorescent sterol dyes by endothelial cells; however, whether this endocytic route corresponds to the AMF uptake pathway remains to be determined (35).

Cholesterol could impact indirectly on macropinocytosis through modulation of phosphatidylinositol 4,5-biphosphate-dependent reorganization of the actin cytoskeleton (13, 36). AMF uptake was not affected by disruption of the actin cytoskeleton with cytochalasin D in MDA-435 cells (Fig. 7) or MCF7 cells (data not shown). Actin cytoskeleton disruption is associated with increased mobility of Cav1 and caveolae-mediated uptake (37–41). The independence of AMF uptake on actin cytoskeleton integrity further distinguishes this pathway from caveolae-mediated endocytosis.

We have shown previously that AMF uptake to the smooth endoplasmic reticulum is distinct from raft-dependent cholera toxin b-subunit uptake to the Golgi apparatus and SV40 uptake to the endoplasmic reticulum (11). The PI3K dependence and actin independence of AMF internalization provide further evidence for the distinct nature of this dynamin-dependent, raft-dependent pathway. Of particular importance, this pathway is shown here to be tumor cell-specific and associated with enhanced AMFR expression in aggressive tumor cells.

AMF-dependent p-Akt activation in MDA-435 cells and PI3K-dependent AMF uptake is indicative of a feedback loop between these two cancer-related proteins functionally linking the extensive correlation of AMFR and p-Akt in the breast tumor TMA. Stable transfection of NIH-3T3 fibroblasts with AMF, resulting in autocrine activation of AMFR, neoplastic transformation, and resistance to apoptosis, was found to be associated with Akt activation and reduced Cav1 expression (16). Autocrine activation of AMFR and downstream PI3K signaling in tumor cells may function to generally enhance AMFR trafficking and plasma membrane turnover. Akt activation is generally associated with increased tumor progression and tumor cell invasivity (42) and is an indicator of aggressive tumor behavior and reduced overall survival in node-negative breast cancer (43). Overall AMFR positivity in breast carcinomas did not correlate with patient disease-specific survival, as reported for p-Akt labeling of the same TMA (24). This is consistent with a recent study of AMF and AMFR expression in breast tumors (44). Coordinate overexpression of AMFR and p-Akt may define a cohort of human breast cancers that, although not the most clinically aggressive, does represent a significant proportion of all invasive tumors.

Although factors other than Cav1 and p-Akt may regulate AMF uptake, our data suggest that internalization of cell surface AMFR may be associated with PI3K-dependent activation of Akt and reduction of Cav1 levels in breast tumor cells. In our invasive breast cancer patient cohort, AMFR tumor expression showed no significant correlation with ER or HER2 expression, but it did present a negative correlation with PR expression. Thus, individuals with breast tumors expressing AMFR may represent a specific subset of patients with breast cancer who may have little benefit from HER2 targeted or hormonal therapies. The abundant expression of AMFR by cancer cells *in vitro* and *in vivo* suggests that the dynamin and PI3K-dependent, Cav1-regulated, raft-mediated endocytosis of AMF may represent a cancer cell-specific endocytic pathway.

Acknowledgment—We thank Mohammad Amraei for assistance.

REFERENCES

1. Watanabe, H., Takehana, K., Date, M., Shinozaki, T., and Raz, A. (1996) *Cancer Res.* **56,** 2960–2963
2. Hirono, Y., Fushida, S., Yonemura, Y., Yamamoto, H., Watanabe, H., and Raz, A. (1996) *Br. J. Cancer* **74,** 2003–2007
3. Nakamori, S., Watanabe, H., Kameyama, M., Imaoka, S., Furukawa, H., Ishikawa, O., Sasaki, Y., Kabuto, T., and Raz, A. (1994) *Cancer* **74,** 1855–1862
4. Otto, T., Birchmeier, W., Schmidt, U., Hinke, A., Schipper, J., Rübben, H., and Raz, A. (1994) *Cancer Res.* **54,** 3120–3123
5. Maruyama, K., Watanabe, H., Hitoshi, S., Takayama, T., Gofuku, J., Yano, H., Inoue, M., Tamura, S., Raz, A., and Monden, M. (1995) *Int. J. Cancer* **64,** 316–321
6. Nagai, Y., Ishikawa, O., Miyachi, Y., and Watanabe, H. (1996) *Dermatology* **192,** 8–11
7. Takanami, I., Takeuchi, K., Naruke, M., Kodaira, S., Tanaka, F., Watanabe, H., and Raz, A. (1998) *Tumor Biol.* **19,** 384–389
8. Taniguchi, K., Yonemura, Y., Nojima, N., Hirono, Y., Fushida, S., Fujimura, T., Miwa, K., Endo, Y., Yamamoto, H., and Watanabe, H. (1998) *Cancer* **82,** 2112–2122
9. Sjoblom, T., Jones, S., Wood, L. D., Parsons, D. W., Lin, J., Barber, T., Mandelker, D., Leary, R. J., Ptak, J., Silliman, N., Szabo, S., Buckhaults, P., Farrell, C., Meeh, P., Markowitz, S. D., Willis, J., Dawson, D., Willson, J. K. V., Gazdar, A. F., Hartigan, J., Wu, L., Liu, C., Parmigiani, G., Park, B. H., Bachman, K. E., Papadopoulos, N., Vogelstein, B., Kinzler, K. W., and Velculescu, V. E. (2006) *Science* **314,** 268–274
10. Benlimame, N., Le, P. U., and Nabi, I. R. (1998) *Mol. Biol. Cell* **9,** 1773–1786
11. Le, P. U., and Nabi, I. R. (2003) *J. Cell Sci.* **116,** 1059–1071
12. Le, P. U., Guay, G., Altschuler, Y., and Nabi, I. R. (2002) *J. Biol. Chem.* **277,** 3371–3379
13. Kirkham, M., and Parton, R. G. (2005) *Biochim. Biophys. Acta* **1745,** 273–286
14. Lajoie, P., and Nabi, I. R. (2007) *J. Cell Mol. Med.* **11,** 644–653
15. Pelkmans, L., Kartenbeck, J., and Helenius, A. (2001) *Nat. Cell Biol.* **3,** 473–483
16. Tsutsumi, S., Hogan, V., Nabi, I. R., and Raz, A. (2003) *Cancer Res.* **63,** 242–249
17. Nabi, I. R., Watanabe, H., and Raz, A. (1990) *Cancer Res.* **50,** 409–414
18. Yu, D., Jia, W. W., Gleave, M. E., Nelson, C. C., and Rennie, P. S. (2004) *Prostate* **59,** 370–382
19. Joshi, B., Ordonez-Ercan, D., Dasgupta, P., and Chellappan, S. (2005) *Oncogene* **24,** 2204–2217
20. Altschuler, Y., Liu, S., Katz, L., Tang, K., Hardy, S., Brodsky, F., Apodaca, G., and Mostov, K. (1999) *J. Cell Biol.* **147,** 7–12
21. Parker, R. L., Huntsman, D. G., Lesack, D. W., Cupples, J. B., Grant, D. R., Akbari, M., and Gilks, C. B. (2002) *Am. J. Clin. Pathol.* **117,** 723–728
22. Reiner, A., Neumeister, B., Spona, J., Reiner, G., Schemper, M., and Jakesz, R. (1990) *Cancer Res.* **50,** 7057–7061
23. Wiseman, S. M., Makretsov, N., Nielsen, T. O., Gilks, B., Yorida, E., Cheang, M., Turbin, D., Gelmon, K., and Huntsman, D. G. (2005) *Cancer* **103,** 1770–1777
24. Sutherland, B. W., Kucab, J., Wu, J., Lee, C., Cheang, M. C. U., Yorida, E., Turbin, D., Dedhar, S., Nelson, C., Pollak, M., Leighton Grimes, H., Miller, K., Badve, S., Huntsman, D., Blake-Gilks, C., Chen, M., Pallen, C. J., and Dunn, S. E. (2005) *Oncogene* **24,** 4281–4292
25. Liu, C. L., Prapong, W., Natkunam, Y., Alizadeh, A., Montgomery, K., Gilks, C. B., and van de Rijn, M. (2002) *Am. J. Pathol.* **161,** 1557–1565
26. Amyere, M., Payrastre, B., Krause, U., Smissen, P. V. D., Veithen, A., and Courtoy, P. J. (2000) *Mol. Biol. Cell* **11,** 3453–3467
27. Araki, N., Hatae, T., Furukawa, A., and Swanson, J. A. (2003) *J. Cell Sci.* **116,** 247–257
28. Zhou, K., Pandol, S., Bokoch, G., and Traynor-Kaplan, A. E. (1998) *J. Cell Sci.* **111,** 283–294

29. Goetz, J. G., and Nabi, I. R. (2006) *Biochem. Soc. Trans.* **340,** 370–373
30. Fang, S., Ferrone, M., Yang, C., Jensen, J. P., Tiwari, S., and Weissman, A. M. (2001) *Proc. Natl. Acad. Sci. U. S. A.* **98,** 14422–14427
31. De Larco, J. E., Wuertz, B. R., Rosner, K. A., Erickson, S. A., Gamache, D. E., Manivel, J. C., and Furcht, L. T. (2001) *Am. J. Pathol.* **158,** 639–646
32. Watanabe, H., Nabi, I. R., and Raz, A. (1991) *Cancer Res.* **51,** 2699–2705
33. Nabi, I. R., and Le, P. U. (2003) *J. Cell Biol.* **161,** 673–677
34. Pelkmans, L., Fava, E., Grabner, H., Hannus, M., Habermann, B., Krausz, E., and Zerial, M. (2005) *Nature* **436,** 78–86
35. Niles, W. D., and Malik, A. B. (1999) *J. Membr. Biol.* **167,** 85–101
36. Kwik, J., Boyle, S., Fooksman, D., Margolis, L., Sheetz, M. P., and Edidin, M. (2003) *Proc. Natl. Acad. Sci. U. S. A.* **100,** 13964–13969
37. Conrad, P. A., Smart, E. J., Ying, Y.-S., Anderson, R. G. W., and Bloom, G. S. (1995) *J. Cell Biol.* **131,** 1421–1433
38. Parton, R. G., Joggerst, B., and Simons, K. (1994) *J. Cell Biol.* **127,** 1199–1215
39. Thomsen, P., Roepstorff, K., Stahlhut, M., and van Deurs, B. (2002) *Mol. Biol. Cell* **13,** 238–250
40. Mundy, D. I., Machleidt, T., Ying, Y.-S., Anderson, R. G. W., and Bloom, G. S. (2002) *J. Cell Sci.* **115,** 4327–4339
41. Pelkmans, L., Puntener, D., and Helenius, A. (2002) *Science* **296,** 535–539
42. Nicholson, K. M., and Anderson, N. G. (2002) *Cell. Signal.* **14,** 381–395
43. Schmitz, K. J., Otterbach, F., Callies, R., Levkau, B., Holscher, M., Hoffmann, O., Grabellus, F., Kimmig, R., Schmid, K. W., and Baba, H. A. (2004) *Mod. Pathol.* **17,** 15–21
44. Jiang, W. G., Raz, A., Douglas-Jones, A., and Mansel, R. E. (2006) *J. Histochem. Cytochem.* **54,** 231–241

Raft-dependent Endocytosis of Autocrine Motility Factor Is Phosphatidylinositol 3-Kinase-dependent in Breast Carcinoma Cells

Liliana D. Kojic, Bharat Joshi, Patrick Lajoie, Phuong U. Le, Michael E. Cox, Dmitry A. Turbin, Sam M. Wiseman and Ivan R. Nabi

J. Biol. Chem. 2007, 282:29305-29313.
doi: 10.1074/jbc.M704069200 originally published online August 8, 2007
